International Center for
Quantum-field Measurement Systems for
Studies of the Universe and Particles
WPI research center at KEK

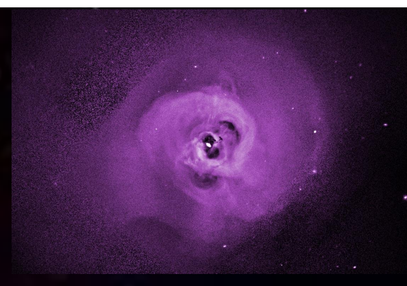

Sensitivity Study for Astrophysical Limits on Axion-like Particles with XRISM/Resolve and Future X-ray Observatories

Yu Zhou, Jiejia Liu, Volodymyr Takhistov, and Kazuhisa Mitsuda

Axion-like particles (ALPs) constitute well-motivated dark matter (DM) candidates and naturally appear in theories beyond the Standard Model. ALP-photon interactions facilitate conversion of X-ray signals into ALPs propagating through astrophysical magnetic fields. Active galactic nuclei (AGNs) are especially promising targets for sensitive tests of photon-ALP couplings, since ALP-induced oscillation features can be easily distinguished from the source emission spectra. We systematically analyze ALP-photon conversion in three distinct systems: (1) background AGNs at a line-of-sight passing through a foreground intracluster magnetic field, (2) central AGNs whose line-of-sight passes through the magnetic field of its own DM halo, (3) Galactic X-ray sources interacting with Milky Way's magnetic field. We establish the ALP-photon coupling sensitivity reach considering observations of the recently launched X-ray telescope XRISM as well as future detectors such as Athena and Arcus. The impact of uncertainties of the magnetic field and photon statistics on constraining photon-axion conversion is discussed.

Keywords: Axion-like particle — X-rays: cluster— AGN

Photon-ALP conversion in the perpendicular magnetic field

- Axion-like particles (ALPs)
  - very light pseudo-scalar spin-zero bosons a characterized by a two-photon coupling
  - generalization of the axion
    - Axion : the pseudo-Goldstone boson associated with the Peccei-Quinn symmetry proposed as a natural solution to the strong CP problem

- Photon-ALP mixing : takes place in the presence of an external electromagnetic field and leads to
  - photon-ALP oscillations
  - the change of the polarization state of photons traveling in a magnetic field

- The equation of motion describing the ALP-photon interconversion :

$$\left(\omega + \begin{pmatrix} \Delta_\gamma & \Delta_F & \Delta_{\gamma ax} \\ \Delta_F & \Delta_\gamma & \Delta_{\gamma ay} \\ \Delta_{\gamma ax} & \Delta_{\gamma ay} & \Delta_a \end{pmatrix} - i\partial_z \right) \begin{pmatrix} |\gamma_x\rangle \\ |\gamma_y\rangle \\ |a\rangle \end{pmatrix} = 0,$$

ω : energy of the photon or ALP
$|\gamma_x\rangle$ and $|\gamma_x\rangle$: two photon polarizations
a : ALP mass $\Delta_{\gamma ai} = \frac{g_{a\gamma\gamma} B_i}{2}$: mixing term
$\Delta_\gamma = -\frac{\omega_{pl}^2}{2\omega}$: photon mass term, $\omega_{pl} = \sqrt{4\pi\alpha n_e / m_e}$
$\Delta_a = -\frac{m_a^2}{\omega}$: ALP mass term
$\Delta_F = 0$: Faraday rotation term, negligible for X-rays

Astrophysical systems for testing photon-ALP conversion

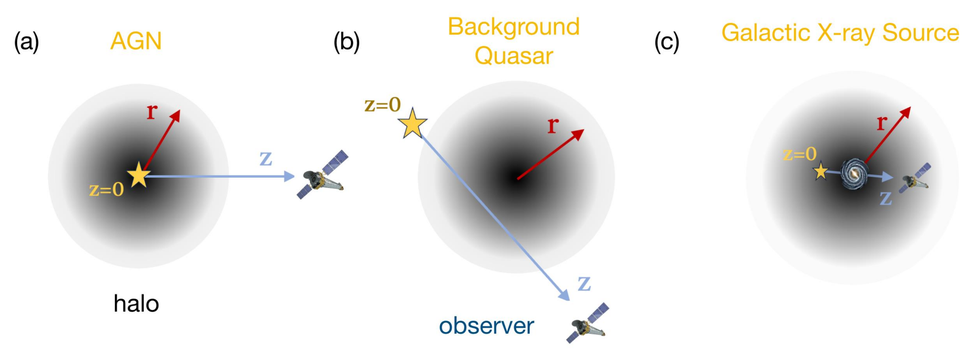

Table 1. Basic information of the three astrophysical systems investigated in this study.

Type	Central AGN - galaxy cluster	Background Quasar - galaxy cluster	Galactic X-ray binary - Milky Way
Photon Background Source	NGC 1275	SDSS J162906.84+393240.5	4U 1820-30
Source Flux (2-10 keV)	2.209×10^{-9} $ergs\ cm^{-2}\ s^{-1}$	1.0745×10^{-13} $ergs\ cm^{-2}\ s^{-1}$	5.0048×10^{-9} $ergs\ cm^{-2}\ s^{-1}$
Magnetic Field Source	Perseus Cluster	Abell 2199	Milky Way
Maximum B-field Magnitude along the source line-of-sight	8 (μG)	0.4 (μG)	3 (μG)
Illustration in Figure 2	(a)	(b)	(c)

First column: the brightest AGN that resides in the galaxy cluster center; Second column: the brightest background quasar with its line-of-sight that cuts through the outskirt of a galaxy cluster in the foreground; Third column: two galactic X-ray binary systems that are most likely to be suitable for this work given combined considerations of their location respective to the galactic plane, distance to the Earth, flux, and simplicity of the energy spectrum.

Magnetic field, electron density, and the plasma frequency of the systems

Perseus cluster | **Abell 2199** | **Milky Way** (YMW16 model)

- Magnetic field : $B(z) = B_0 \left[\frac{n_e(z)}{n(R_0)}\right]^\alpha$ — R_0 = 25 kpc, B_0 = 7.5 μG, and α = 0.5 (Fabian et al. 2006)
- Electron density : $n_e(z) = \frac{3.9\times10^{-2}}{[1+(z/80\ \mathrm{kpc})^2]^{1.8}}\mathrm{cm}^{-3} + \frac{4.05\times10^{-3}}{[1+(z/280\ \mathrm{kpc})]^{0.87}}\mathrm{cm}^{-3}$ — $n(R_0)$ = 0.101 cm^{-3}, B_0 = 11.7 μG, and α = 0.9 (Vacca et al. 2012)
- Plasma frequency : $\omega_{pl} = \sqrt{4\pi\alpha n_e / m_e}$ — Churazov et al. (2003)

$n_e(r) = n_{0_{\rm int}}\left(1+\frac{r^2}{r_{\rm c_{int}}^2}\right)^{-\frac{3}{2}\beta_{\rm int}} + n_{0_{\rm ext}}\left(1+\frac{r^2}{r_{\rm c_{ext}}^2}\right)^{-\frac{3}{2}\beta_{\rm ext}}$

Parameter	Value	Units
$\beta_{\rm int}$	$1.5^{+0.2}_{-0.5}$	
$r_{\rm c_{int}}$	9^{+2}_{-3}	kpc
$n_{0_{\rm int}}$	$0.074^{+0.004}_{-0.01}$	cm^{-3}
$\beta_{\rm ext}$	$0.39^{+0.01}_{-0.03}$	
$r_{\rm c_{ext}}$	$26.0^{+0.8}_{-0.6}$	kpc
$n_{0_{\rm ext}}$	$0.027^{+0.003}_{-0.003}$	cm^{-3}

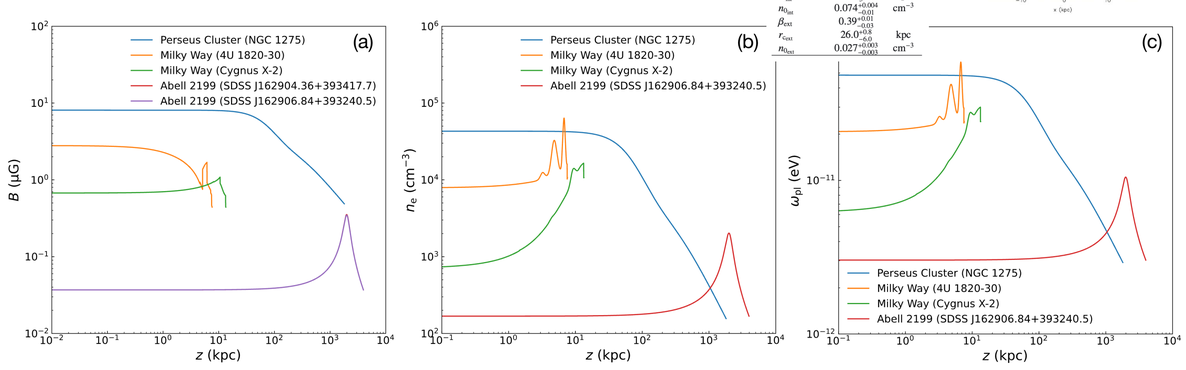

Background energy spectrum and the absorption caused by photon-ALP conversion

An example of the photon survival probability model fit to the background AGN energy spectrum (NGC 1275)

Simulation data assuming XRISM/Resolve 5 Ms observation

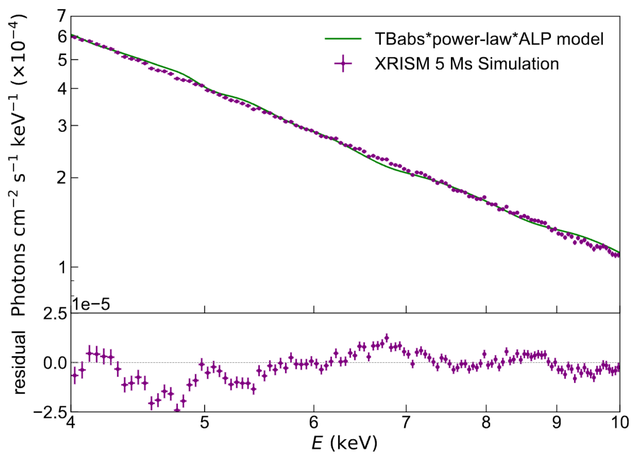

Examples of the photon survival probability curves for given photo-ALP coupling coefficient $g_{a\gamma\gamma}$ and ALP mass m_a
(resonance solution in Marsh et al 2017)

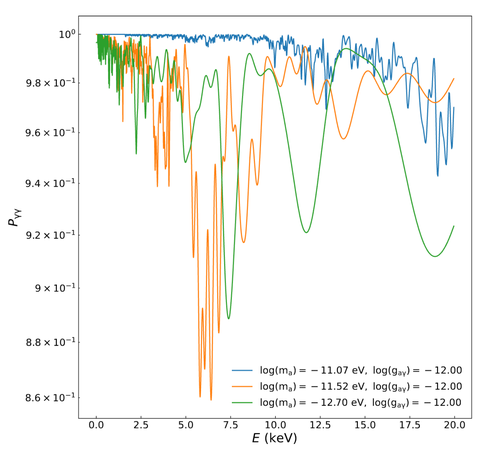

Photon-ALP conversion probability curves averaged for turbulent magnetic fields

- The magnetic field along the line of sight is modeled as a series of cells of extent Δz.
- Model 1 : draw coherence lengths randomly from (1+r/50 kpc)×3.5 kpc to (1+r/50 kpc)×10 kpc, with a power-law fall-off as p(Δz) μ $\Delta z^{-1.2}$ since coherence lengths are expected to grow with distance from the cluster center.
- Model 2 : the value of Δz is chosen according to a probability distribution function p(Δz), typically a power law, p(Δz) μ $\Delta z^{-1.2}$ spanning 3.5–10 kpc.

Model	N	B-Field	Λ_c Scaling?	$\beta_{pl}(z)$	Range of Scales (kpc)
1	200	Cell-based	Yes	Constant, 100	3.5–10
2	200	Cell-based	No	Constant, 100	3.5–10

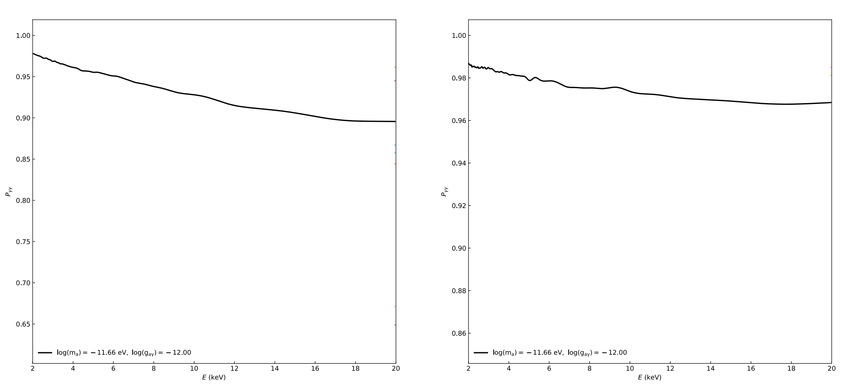

Sensitivity of photon-ALP conversion coefficient using XRISM/Athena/Arcus

	Energy resolution	Effective area	Spatial resolution	Field of view
• XRISM / Resolve :	≤ 7 eV FWHM @ 6keV	≥ 210 cm² @ 6 keV	≤ 1.7 arcmin	≥ 2.9 x 2.9 arcmin²
• Athena / X-IFU :	3 eV	1.4 square meters at 1 keV	5 arcseconds on-axis	40' x 40'
• Arcus / grating :	resolving power of R > 3000 (12–50 Å)	> 200 cm²	1.4~10 arc seconds	—

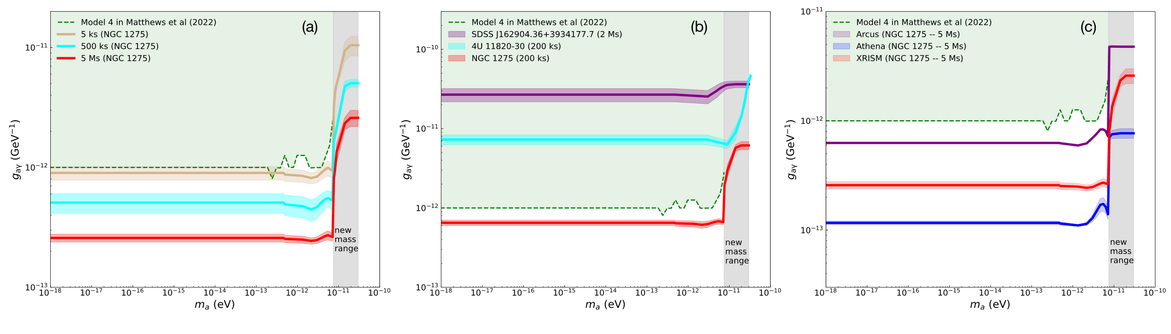

Sensitivity of photon-ALP conversion coefficient dependence on binning factor

- Dependence on energy resolution : we create response files for detectors assuming an energy resolution of 1 eV, 10 eV, and 100 eV.
- Dependence on binning factor : binning the energy channels of the energy spectrum for fitting (more channels per bin —> higher statistics and less error of data per bin)
- Dependence on the ALP energy relative to photon : massless ($m_a \ll \omega_{pl}$), resonance ($m_a \sim \omega_{pl}$), massive ($m_a \gg \omega_{pl}$)

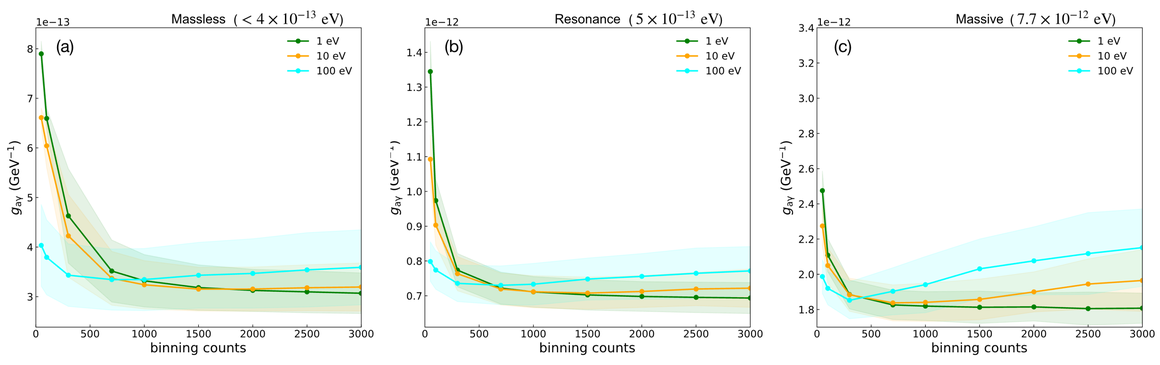

Catalogue of the background quasar

srcID	QSO Name	RA (deg)	Dec (deg)	$z_{\rm QSO}$	$\log F_{\rm X,0.3-10}$ (erg cm^{-2} s^{-1})	GlC Name	$z_{\rm GlC}$
1	SDSS J125859.27+275308.5	194.746958	27.885694	1.13507 ± 0.00210 [1]	$-13.22^{+0.12}_{-0.17}$		
2	SDSS J125915.61+280804.8	194.815042	28.134667	2.07844 ± 0.00048 [2]	$-13.51^{+0.33}_{-0.17}$		
3	SDSS J125831.74+275330.2	194.632250	27.891722	1.14093 ± 0.00021 [2]	$-13.19^{+0.11}_{-0.08}$		
4	QSO B1258+280	195.294292	27.816417	1.93000 [3]	$-13.17^{+0.03}_{-0.03}$	A1656	0.02340 [10]
5	2XMM J125926.2+282332	194.859167	28.392222	1.15350 [4]	$-12.77^{+0.02}_{-0.02}$		
6	QSO B1258+2835	195.253583	28.329094	1.36102 ± 0.00013 [2]	$-12.93^{+0.02}_{-0.02}$		
7	QSO B1258+2839	195.200417	28.389094	1.92348 ± 0.00014 [2]	$-12.86^{+0.02}_{-0.02}$		
8	SDSS J005606.43-011958.4	14.026833	-1.332911	0.84041 ± 0.00011 [5]	$-13.35^{+0.04}_{-0.05}$	A119	0.04450 [10]
9	SDSS J162829.75+392115.1	247.123958	39.354194	0.38268 [9]	$-12.90^{+0.03}_{-0.03}$		
10	[VV2006] J162855.6+394034	247.231667	39.676111	1.51981 ± 0.00033 [2]	$-12.88^{+0.05}_{-0.03}$		
11	SDSS J162806.89+393911.0	247.028708	39.653056	1.16366 [6]	$-13.47^{+0.11}_{-0.10}$		
12	SDSS J162809.81+392814.7	247.040875	39.470750	1.15857 [6]	$-13.23^{+0.03}_{-0.03}$	A2199	0.03090 [10]
13	SDSS J162904.36+393417.7	247.268167	39.571583	0.95498 [6]	$-12.71^{+0.02}_{-0.02}$		
14	SDSS J162906.84+393240.5	247.278500	39.544583	0.78300 [5]	$-12.81^{+0.02}_{-0.02}$		
15	[VV2006] J162937.1+394100	247.404583	39.683333	0.72375 ± 0.00010 [7]	$-12.93^{+0.03}_{-0.04}$		
16	SDSS J233831.66+270035.0	354.631958	27.009731	1.64859 [6]	$-13.12^{+0.08}_{-0.09}$	A2634	0.03120 [11]
17	SDSS J233820.00+265638.7	354.583358	26.944089	1.28827 [6]	$-13.01^{+0.06}_{-0.07}$		
18	SDSS J012555.11-012925.1	21.479625	-1.490306	2.65800 [5]	$-14.18^{+1.01}_{-0.37}$		
19	SDSS J012556.54-012731.8	21.485583	-1.458833	2.80773 ± 0.00016 [7]	$-14.09^{+0.54}_{-0.28}$	A194	0.01780 [11]
20	SDSS J012610.47-012605.0	21.543625	-1.434722	1.06317 ± 0.00040 [5]	$-13.62^{+0.08}_{-0.42}$		
21	SDSS J012556.71-012607.7	21.486250	-1.435472	1.88712 ± 0.00054 [5]	$-14.03^{+0.42}_{-0.24}$		
22	UGC12064	337.835792	39.358222	0.01711 ± 0.00015 [8]	$-12.92^{+0.01}_{-0.09}$	3C449	0.01711 ± 0.00015 [8]
23	2XMM J083107.3+654653	127.780417	65.781389	0.63800 [9]	$-12.80^{+0.02}_{-0.02}$	A665	0.01860 [11]